JURNAL KIMIA VALENSI
p-ISSN: 2460-6065; e-ISSN: 2548-3013
Journal homepage: https://journal.uinjkt.ac.id/index.php/valensi
Research Article

The Synthesis of Y-zeolite-modified $CaCO_3$-ZnO Nanocomposites as an Antibacterial Agent

Maysa Artissiani[1], Nuni Widiarti[1*], Sri Wahyuni[1], Endah Widhihastuti[2], Neli Syahida Ni'ma[2]

[1]*Department of Chemistry, Faculty of Mathematics and Natural Science, Universitas Negeri Semarang, Semarang, 50229, Indonesia*
[2]*Department of Pharmacy, Faculty of Medicine, Universitas Negeri Semarang, Semarang, 50237, Indonesia*

Email: nuni_kimia@mail.unnes.ac.id

Article Info
Received: Dec 03, 2023
Revised: Dec 12, 2024
Accepted: May 07, 2024
Online: June 11, 2024

Citation:
Artissiani, M., Widiarti, N., Wahyuni, S., Widhiastuti, E., & Ni'ma, N. S. (2024). The Synthesis of Y-zeolite-modified $CaCO_3$-ZnO Nanocomposites as an Antibacterial Agent. *Jurnal Kimia Valensi*, *10*(1), 145 - 154.

Doi:
10.15408/jkv.v10i1.36246

Abstract
The ability of inorganic antibacterial agents like metal oxides and nanoscale inorganic materials to inhibit bacterial growth rates has yet to receive much research attention. In this study, $CaCO_3$-ZnO/Y-zeolite nanocomposites were created utilizing coprecipitation and impregnation techniques with $Ca(CH_3COO)_2$, $Zn(CH_3COO)_2{\cdot}2H_2O$, Y-zeolite precursors. Physical and chemical characteristics of nanocomposites have been investigated using XRD, FTIR, and SEM-EDX characterizations. The agar-well diffusion method tested the substance for antibacterial activity against gram-positive and gram-negative bacteria. Nanocomposites have a crystal size range of 35.46-36.53 nm and a crystallinity of 35-37 %, according to the results of XRD analysis. The carbonate groups are visible in FTIR data at wave numbers 1433, 875, and 712 cm^{-1}. The Zn-O absorption band was verified at wave numbers 600-400 cm^{-1}. The Y-zeolite absorption bands at wave numbers 1012-997 cm^{-1} and 745-746 cm^{-1} were confirmed. The particle morphology is cube-shaped with irregular sizes. The EDX result showed that the composition consists of 35.92 % calcium, 1.68 % zinc, 44.81 % oxygen, and 13.79 % carbon as elements. With the addition of 2.5 % Y-zeolite, the antibacterial activity of nanocomposites showed the best results, with an inhibition zone diameter of 7.62 mm against *Escherichia coli* and 6.56 mm against *Staphylococcus aureus* bacteria.

Keywords: antibacterial; calcium carbonate; nanocomposite; Y-zeolite; zinc oxide

1. INTRODUCTION

The emergence of resistant microbes and persistent bacterial infections are recognized as serious public health problems. It can affect populations in developing countries as well as low- and middle-income countries [1]. Therefore, in order to prevent and control these pathogens, it is necessary to carry out early diagnosis and appropriate treatment procedures. In this regard, nanomaterial-based therapies have received a great deal of interest in the scientific community due to their favorable antibacterial properties. Nanocomposites have unique properties, such as a high surface-to-volume ratio and antibacterial properties that outperform micron-sized materials [2].

Antibacterial agents are divided into two types: organic and inorganic. The fundamental issue with commonly used organic antibacterial agents is their low stability at relatively high temperatures and pressures, whereas inorganic antibacterial agents are highly stable and powerful [3]. Organic antibacterial agents have environmentally hazardous activities along with a limited usage period, so it is preferable to use inorganic antibacterial agents since these substances are safe for the environment and easy to use [4].

ZnO is a multifunctional inorganic material with effective antibacterial activity. One of the applications of ZnO is in the food packaging industry because it is non-toxic, has antibacterial and antifungal properties, and has high photochemical and catalytic activity [5]. As an antibacterial, ZnO has a mechanism of action that inhibits cell synthesis, damages bacterial cell walls, and interferes with cell metabolism [6]. ZnO in the form of nanoparticles can inhibit growth rates of gram-positive bacteria such as *Staphylococcus aureus* [7].

Calcium carbonate ($CaCO_3$) is an inorganic mineral used as a filler in chemical industries such as toothpaste, paper, and paint. There are three types of crystalline forms of calcium carbonate: calcite, aragonite, and vaterite. Calcite with rhombohedral shapes includes stable phases at room temperature, while aragonite and vaterite are stabilizing phases that can transform into stable stages [8]. Calcium carbonate in the form of calcite has many applications in the field of health, such as a nutritious calcium booster and as an antiacid for the stomach [9]. Based on the production process, calcium carbonate is divided into two types: heavy and light. The heavy type is produced through the milling process of calcium stones with a high $CaCO_3$ composition. The light type is manufactured through the process of precipitation resulting from chemical reactions so that calcium carbonate of high purity is obtained [10]. Precipitate calcium carbonate (PCC) is a calcium carbonate deposit resulting from the reaction of natural materials such as dolomite, calcite, limestone, and marble [11]. The use of PCC as an antibacterial agent offers great opportunities due to its compatible material, biodegradability, and small particle size.

Previous research has explored the antibacterial activity of combining two inorganic materials such as CuO-ZnO [3], ZnO-MgO [12], $CaCO_3$-MgO [13], and $CaCO_3$-ZnO [9]. The CuO-ZnO nanocomposite synthesized using the sol-gel method showed antibacterial activity with an inhibition zone diameter of 2.1 mm against *Staphylococcus aureus* bacteria and 2.3 mm against *Escherichia coli* bacteria [14]. $CaCO_3$-MgO nanocrystals synthesized using the mixing method with calcination at 800 ^oC have the potensial as an antibacterial agent because $CaCO_3$-MgO nanocrystals have a crystal size between 61.85-66.11 nm which can inhibit antibacterial activity [13]. The combination of inorganic materials including ZnO and $CaCO_3$ with stabilizer is expected to produce products with nanocrystal size and good antibacterial activity against *Escherichia coli* and *Staphylococcus aureus*. Several researchers have used zeolite as a stabilizer and promoter. Zeolite is used as a material to promote and stabilize both metals and metal oxides by controlling the size of nanoscale particles. The synthesized CuO-ZnO nanocomposite with zeolite as an agent successfully controls nanoscale particle size [15]. Y-zeolite is chosen as a stabilizer because it has a large Si/Al ratio compared to type A and X-zeolites. A high Si/Al ratio on zeolite produces zeolites with good stability and a large surface area [16].

The agar-well diffusion method is a method of testing antibacterial activity by making holes in an agar medium containing test bacteria. Then the holes are injected with the samples to be tested. After the incubation process, bacterial growth was observed in the inhibition area around the hole [17]. The working principle of this diffusion method is that antibacterial compounds diffuse into the agar medium that has been inoculated with test bacteria. The zone of inhibition on microbial growth is characterized by the presence or absence of a clear zone around the hole. The advantage of the agar-well diffusion method compared to the disc diffusion method is that measuring the zone of inhibition in the agar-well diffusion method is easier to do. This is because microbes are active both on the upper and lower surfaces of the nutrient agar [18].

Based on this explanation, this research will synthesize $CaCO_3$-ZnO nanocomposites with a Y-zeolite modifier as a carrier using coprecipitation and impregnation methods. The $CaCO_3$-ZnO/Y-zeolite nanocomposites were tested for antibacterial activity against gram-negative (*Escherichia coli*) and gram-positive (*Staphylococcus aureus*) bacteria.

2. RESEARCH METHODS

Material

The materials used in this study include $Zn(CH_3COO)_2{\cdot}2H_2O$ 98% (Merck), $Ca(CH_3COO)_2$ 94% (Merck), Y-zeolite 90% (Sigma-Aldrich), $H_2C_2O_4{\cdot}2H_2O$ p.a. (Merck), Mc Farland 0.5 solution, distilled water, Nutrient Agar (Merck), *Escherichia coli* bacteria ATCC 25922, and *Staphylococcus aureus* bacteria ATCC 25923.

Synthesis of $CaCO_3$-ZnO Nanocomposites

$CaCO_3$-ZnO nanocomposites were synthesized using the coprecipitation method with modification [19]. $CaCO_3$-ZnO nanocomposites (mole ratio 1:1) were prepared by mixing 50 mL calcium acetate 1 M and 50 mL zinc acetate dihydrate 1 M until homogeneous. Oxalic acid dihydrate solution 0.15 M was added to the mixture until a precipitate formed while stirring for 10 hours at room temperature. The precipitate was collected and washed using distilled water until the pH was equal to the pH of the solvent (pH 5). The precipitate obtained was then dried in an oven for 12 hours at 105 ^oC. The solid was calcined for 5 hours at 600 ^oC in a furnace to obtain a $CaCO_3$-ZnO nanocomposite. The same steps were followed for the preparation of $CaCO_3$-ZnO nanocomposites with mole ratios of 2:1 and 1:2.

Synthesis of $CaCO_3$-ZnO/Y-zeolite Nanocomposites

$CaCO_3$-ZnO/Y-zeolite nanocomposites were synthesized using the coprecipitation method with modification [19]. Comparison of mole ratios in the synthesis of $CaCO_3$-ZnO with the best antibacterial activity modified with Y-zeolite. Calcium acetate and zinc acetate dihydrate solutions were mixed until homogeneous. Y-zeolite at 2.5 % was added to the calcium acetate and zinc acetate mixture. Oxalic acid dihydrate solution was added to the mixture until a precipitate formed while stirring for 10 hours at room temperature. The precipitate was collected and washed using distilled water until the pH was equal to the pH of the solvent (pH 5). The precipitate obtained was then dried in an oven for 12 hours at 105 ºC. The solid was calcined for 5 hours at 600 ºC in a furnace to obtain a $CaCO_3$-ZnO nanocomposite. Furthermore, the same steps were carried out for the addition of Y-zeolite 5 and 10 %.

Characterization

The nanocomposite products ($CaCO_3$-ZnO and $CaCO_3$-ZnO/Y-zeolite) were characterized by FTIR, XRD, and SEM-EDX. Functional group analysis was carried out using PerkinElmer Spectrum IR Version 10.6.1 at wave numbers 4000-400 cm^{-1}. Nanocomposite products were mixed with KBr powders at a ratio of 1:10 and pressed into transparent pellets. X-ray diffraction (XRD) analysis was conducted using X'Pert PRO PANalytical with Cu radiation at a wavelength of 1.5405 Å on 40 kV 30 mA, scanning samples from 10-80 º. Calculation of the crystal size of $CaCO_3$-ZnO and $CaCO_3$-ZnO/Y-zeolite nanocomposites using the Debye-Scherrer equation [20]. The results of the crystal size calculation can be seen in **Table 1**.

$$D \text{ (nm)} = \frac{k \times \lambda}{\beta \times \cos\theta} \quad \dots (1)$$

which D is the average crystal size (nm); k is constant (0.9), λ is the monochromatic wavelength of Cu-Kα (0.54106 nm); β is the full width at half maximum (FWHM) in radians; and theta is the scattering angle (degree).

Scanning Electron Microscopy (SEM) was conducted using FEI Inspect 850 with high-energy electron beam scanning. X-rays in SEM can be used for the identification elemental composition of samples by Energy Dispersive X-ray (EDX) technique. The EDX spectrum was measured by the EDAX-AMETEK detector.

Antibacterial Activity Test

Preparation of bacterial culture

Bacterial stocks were prepared by inoculating one ose of a pure culture of *Escherichia coli* and *Staphylococcus aureus* into nutrient agar, then incubated at 37 ºC for 24 hours.

Preparation of nutrient agar media

As much as 10 grams of nutrient agar were dissolved in 500 mL of distilled water (20 grams/1000 mL). This nutrient agar was used as the base layer and seeding layer. The nutrient agar media that had been homogenized was sterilized using an autoclave at 121 ºC for 15 minutes. Then it was cooled to a temperature of 45–50 °C.

Sterilization of equipment

Petri dishes, cork borer, spatula, and glassware that will be used in the test were sterilized using an autoclave for 15 minutes at 121 ºC.

Preparation of bacterial test

Bacteria were diluted by adding one ose of *Escherichia coli* and *Staphylococcus aureus* bacterial suspensions into each test tube containing 5 mL of a 0.9 % NaCl solution. Then, they were homogenized using a vortex. The turbidity of the bacterial solution should be equal to the turbidity of the 0.5 McFarland solution.

Antibacterial test against Escherichia coli and Staphylococcus aureus

The antibacterial activity of nanocomposites was evaluated using double-layer agar-well diffusion against gram-positive (*Staphylococcus aureus*) and gram-negative (*Escherichia coli*) bacteria [12]. The base layer was made by pouring 25 mL of nutrient agar (NA) solution into a petri dish and allowing it to solidify. The seed layer was prepared by adding 15 mL of bacterial suspension that had been standardized to the 0.5 Mc Farland standard. Next, four wells with a diameter of 5 mm were formed. Then, 0.025 grams of $CaCO_3$-ZnO sample (1:1) was filled in each hole. A petri dish was incubated at 37 ºC for 24 hours. The same process was carried out on $CaCO_3$-ZnO 2:1 and 1:2 as well as on $CaCO_3$-ZnO/Y-zeolite 2.5, 5, and 10 %. The diameter of the clear zone formed was measured using a caliper.

3. RESULTS AND DISCUSSION

Synthesis of $CaCO_3$-ZnO and $CaCO_3$-ZnO/Y-zeolite Nanocomposites

In the synthesis process, zinc acetate dihydrate and calcium acetate were impregnated with zeolite Y to form the complex compound $Ca(C_2O_4)_2Zn$-Y zeolite. The impregnation process aims to attach the active side of the metal to the buffer material [21]. The solid was calcined at 600 ºC for 5 hours to obtain $CaCO_3$-ZnO and $CaCO_3$-ZnO/Y-zeolite nanocomposites. Through the calcination process, complex chemical compounds such as $Ca(C_2O_4)_2Zn$ and $Ca(C_2O_4)_2Zn$-Y zeolite can be dissolved in the presence of heat to form the $CaCO_3$-ZnO and $CaCO_3$-ZnO/Y-zeolite structure. Both the nanocomposite without modification and with Y-zeolite modification produced a white powder.

FTIR Characterization

FTIR spectrophotometer was used to identify the functional groups of $CaCO_3$-ZnO and $CaCO_3$-ZnO/Y-zeolite nanocomposites. FTIR analysis was conducted at wave numbers 4000-400 cm^{-1}, as shown in **Figure 1**.

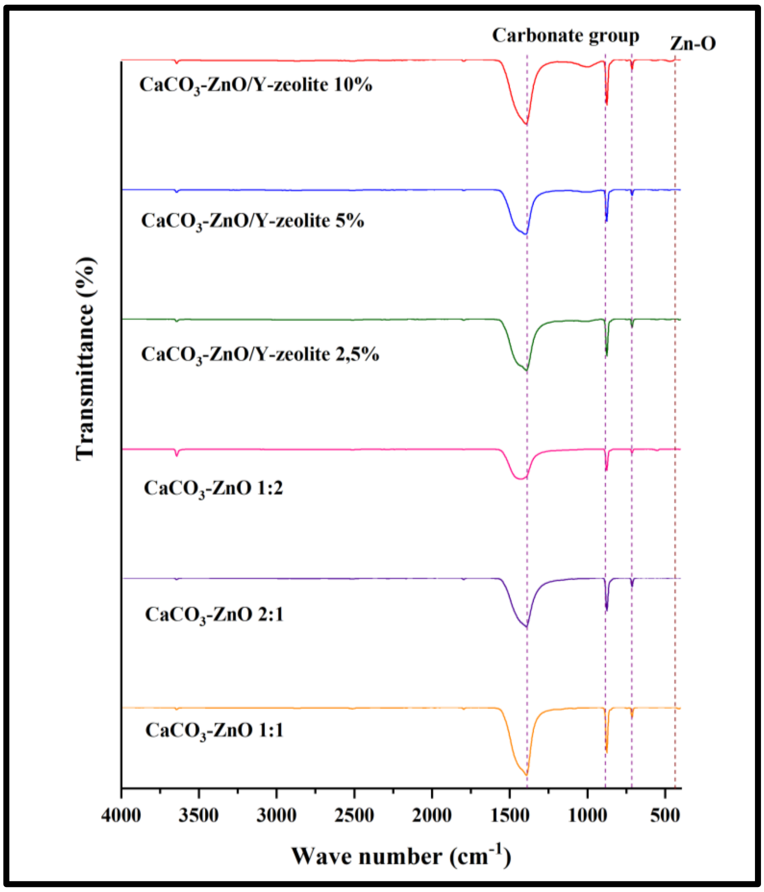

Figure 1. FTIR spectra of $CaCO_3$-ZnO and $CaCO_3$-ZnO/Y-zeolite nanocomposites

The FTIR analysis results in **Figure 1** show the absorption band associated with the stretching vibration of the C-O bond of the carbonate group. The characteristic peaks of $CaCO_3$-ZnO nanocomposites at wave numbers 1433, 875, and 712 cm^{-1} indicate the presence of carbonate groups from $CaCO_3$ compounds [22]. Then, in the $CaCO_3$-ZnO/Y-zeolite nanocomposites, there was a shift of the carbonate groups at wave numbers 1392, 874, and 712 cm^{-1}. The Zn-O absorption band was confirmed at 600-400 cm^{-1} with low peak [23]. There is a shift in the absorption peak along with an increase in the amount of ZnO that is composited. In $CaCO_3$-ZnO/Y-zeolite nanocomposites, asymmetrical absorption bands of Si-O-Si and O-Al-O appear at wave numbers 1012, 1000, and 997 cm^{-1} while symmetrical absorption bands appear at wave numbers 745 and 746 cm^{-1} which are characteristic of Y-zeolite [24]. The absorption tape at wave numbers 720-650 cm^{-1} and 780-720 cm^{-1} is an internal and external T-O symmetrical (Si-O/Al-O) vibration. The absorption of T-O curvature vibrations in a range of wave numbers 475-450 cm^{-1} corresponds to the T-O curve vibrations of the faujasite-type zeolite [25].

XRD Characterization

X-ray diffraction (XRD) analysis was used to analyze the phase and crystal size of the $CaCO_3$-ZnO and $CaCO_3$-ZnO/Y-zeolite nanocomposites. XRD analysis was performed at 2θ angles between 10-80°. The diffractogram of the synthesized nanocomposites can be seen in **Figure 2**.

As a result of the X-ray diffraction analysis (**Figure 2)**, the diffraction patterns were matched with the *Joint Committee on Powder Diffraction Standards* (JCPDS) for comparison. ZnO diffraction patterns appear to peak on 2θ = 31; 34; 36; 56; 72; and 77 ° [26], whereas $CaCO_3$ diffraction patterns appear to peak on 2θ = 23; 29; 39; 43; 47; 48; 57; and 60° [9]. The diffraction pattern of ZnO corresponds to JCPDS 36-1451 with a hexagonal wurtzite structure [27], and $CaCO_3$ corresponds to JCPDS 47-1743 with a rhombohedral crystal structure, the phase of calcite [28]. At a calcination temperature of 600°C, the characteristic peak of $CaCO_3$ has a very high intensity at peak 2θ = 29.4°, indicating the calcite phase. In the $CaCO_3$-ZnO/Y-zeolite nanocomposites, there are characteristic peaks of Y-zeolite shown at 2θ = 26.96; 31.29; and 33.96° by JCPDS 38-0240 [29]. Both in $CaCO_3$-ZnO and $CaCO_3$-ZnO/Y-zeolite nanocomposites, there is a small amount of $CaCO_3$ converted to CaO. This occurs due to the process of releasing CO_2 from $CaCO_3$ to form CaO [30].

Table 1 shows that the $CaCO_3$-ZnO and $CaCO_3$-ZnO/Y-zeolite nanocomposites are already nanosized, less than 100 nm. The $CaCO_3$-ZnO nanocomposite with a mole ratio of 1:2 has the smallest crystal size with large

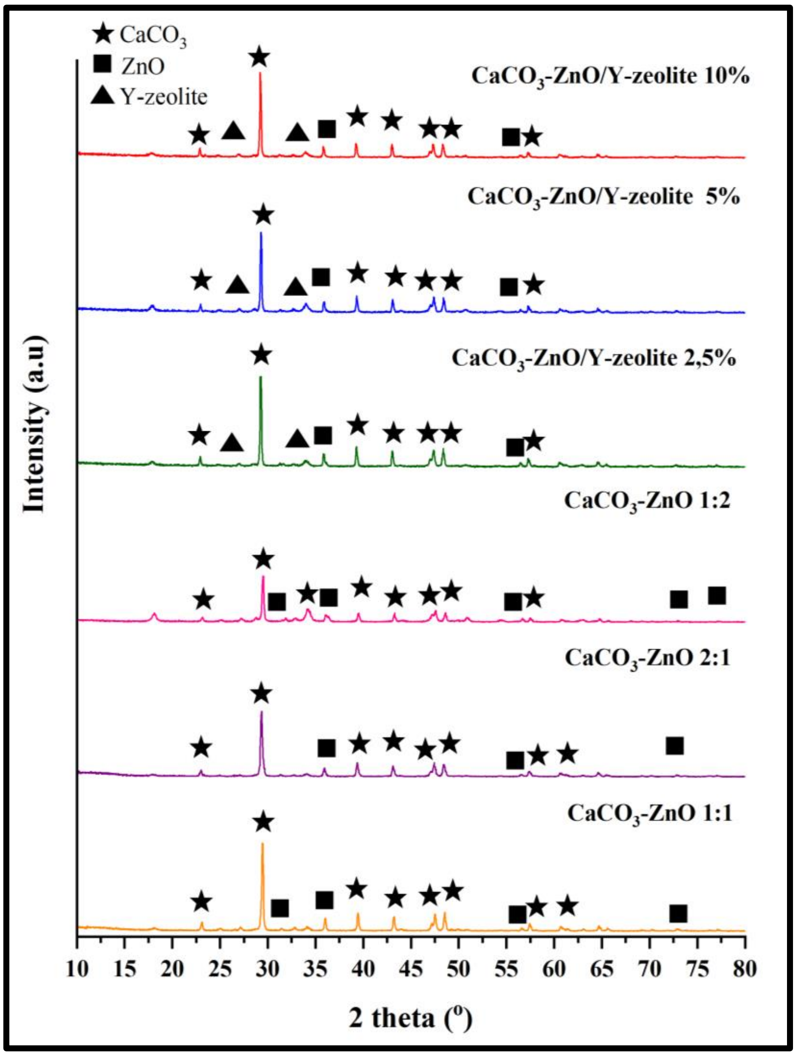

Figure 2. Diffractograms of $CaCO_3$-ZnO and $CaCO_3$-ZnO/Y-zeolite nanocomposites

Table 1. Crystal size and crystallinity of $CaCO_3$-ZnO and $CaCO_3$-ZnO/Y-zeolite

Sample	Crystal size 2θ= 29° (nm)	Crystallinity (%)
$CaCO_3$-ZnO 1:1	31.24	41.54
$CaCO_3$-ZnO 2:1	26.94	42.15
$CaCO_3$-ZnO 1:2	24.04	45.22
$CaCO_3$-ZnO/Y-zeolite 2.5 %	35.46	37.66
$CaCO_3$-ZnO/Y-zeolite 5 %	36.22	37.26
$CaCO_3$-ZnO/Y-zeolite 10 %	36.53	35.03

crystallinity. This shows that the more ZnO that is composited with $CaCO_3$ has an impact on the size of the crystals produced. The combination of ZnO with lower $CaCO_3$ can increase activity as the crystal size decreases. Similar results were reported that $CaCO_3$-ZnO with a mole ratio of 1:2 has better activity[19] compared to the mole ratios 1:1 and 2:1. The crystal size of $CaCO_3$-ZnO was increased after being modified with Y-zeolite. This might be explained by the active sites on $CaCO_3$-ZnO being covered by the presence of Y-zeolite, thus causing an increase in the crystal size of the modified $CaCO_3$-ZnO.

The crystallinity of $CaCO_3$-ZnO was obtained by comparing the area of the crystal with the total area of amorphous and crystalline crystals. The crystallinity of $CaCO_3$-ZnO increases as the amount of added ZnO increases. The addition of ZnO can have a positive effect on the formation of a more regular crystal structure. The peaks shown in the nanocomposites have a high intensity and a clear peak separation pattern. The use of Y-zeolite generally reduces the crystallinity of $CaCO_3$-ZnO. The addition of Y-zeolite in large quantities can reduce the number of active sites due to the closure of the active side by Y-zeolite at high loading, which can reduce crystallinity.

SEM-EDX Characterization

Scanning Electron Microscopy (SEM) analysis was aimed to determine the surface morphology of $CaCO_3$-ZnO and $CaCO_3$-ZnO/Y-zeolite nanocomposites. The results of the surface morphology analysis of $CaCO_3$-ZnO and $CaCO_3$-ZnO/Y-zeolite nanocomposites (**Figure 3**) exhibit cube-like shapes particles with uneven and irregular sizes. This is in accordance with the results confirmed in the FTIR and XRD analyses, which showed the presence of $CaCO_3$ compounds in each sample. In the $CaCO_3$-ZnO 1:1 and 2:1 samples, some particles are bound together as aggregates. In the $CaCO_3$-ZnO 1:2 sample, the aggregate size tends to be smaller and in small quantities. This is in accordance with research conducted by Rahmawati et al. [31], which shows that increasing the molar ratio of Ca/Zn affects increasing the size of agglomerates. Smaller grain and aggregate sizes provide a higher specific surface area [32]. With the addition of 2.5 % Y-zeolite, the aggregate size tends to be smaller than with the addition of 10 % Y-zeolite, which has larger aggregates. This indicates that the more zeolite Y added, the larger the aggregate produced.

Figure 4 shows the results of the elemental composition analysis on $CaCO_3$-ZnO and $CaCO_3$-ZnO/Y-zeolite nanocomposites. The $CaCO_3$-ZnO nanocomposites consist of 45 % calcium, 4.76 % zinc, 42.37 % oxygen, and 7.15 % carbon elements, which indicate the presence of $CaCO_3$ and ZnO compounds [9]. The $CaCO_3$-ZnO/Y-zeolite nanocomposites consist of 35.92 % calcium, 1.68 % zinc, 44.81 % oxygen, 13.79 % carbon, 0.95 % silicon, 1.20 % aluminum, and 1.66 % Y. The confirmed presence of Si, Al, and Y elements indicates that the $CaCO_3$-ZnO/Y-zeolite nanocomposites contain Y-zeolite compounds. Through EDX analysis, the composition of Ca and Zn in the $CaCO_3$-ZnO modified by Y-zeolite changes the composition of the elements formed. Even though the amount is small, it can be seen in the measurement results that it is homogeneous.

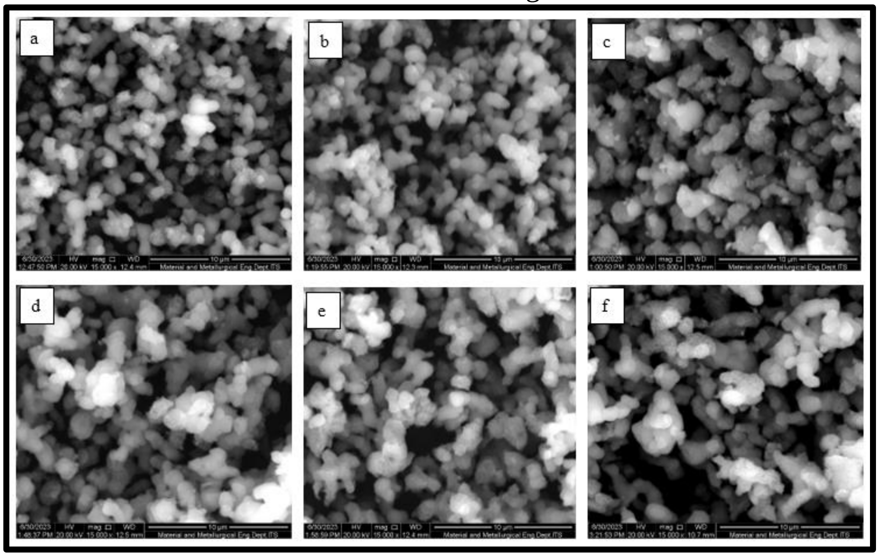

Figure 3. SEM images of $CaCO_3$-ZnO 1:1 (a); 2:1 (b); 1:2 (c), $CaCO_3$-ZnO/Y-zeolite 2.5% (d); 5% (e); and 10% (f)

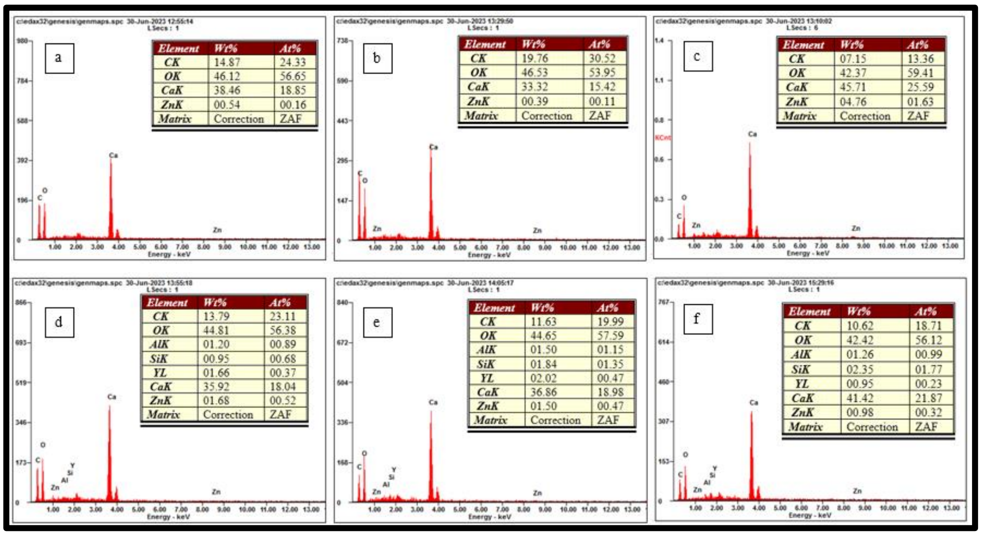

Figure 4. EDX results of $CaCO_3$-ZnO 1:1 (a); 2:1 (b); 1:2 (c), $CaCO_3$-ZnO/Y-zeolite 2.5% (d); 5% (e); and 10% (f)

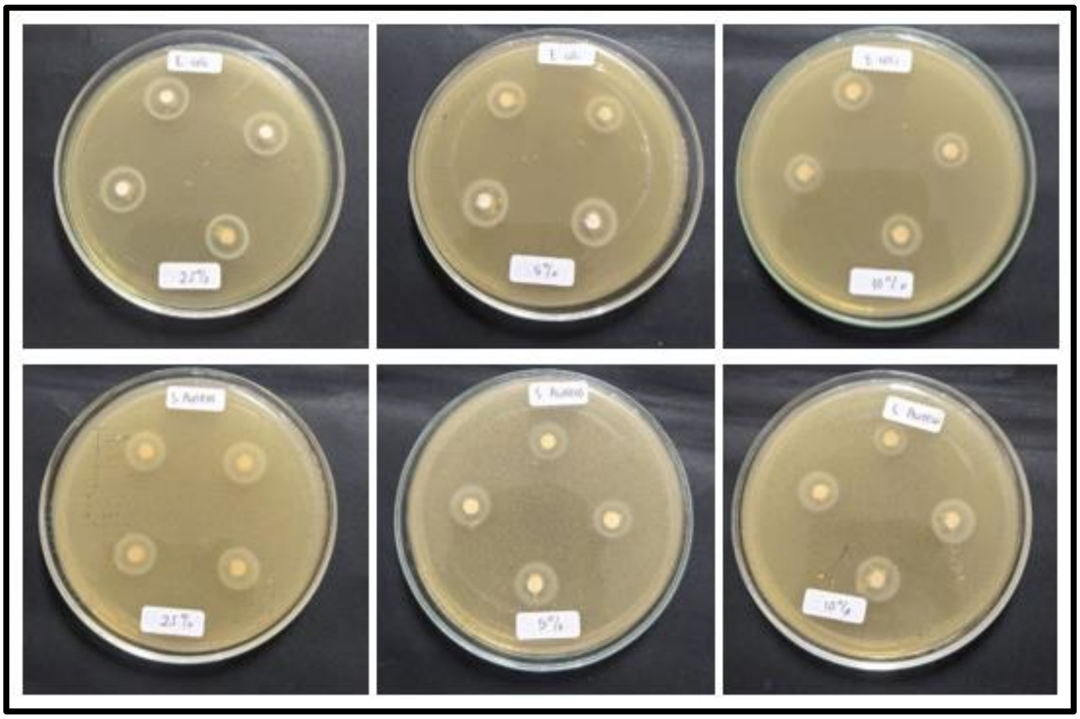

Figure 5. Inhibition zone diameter of $CaCO_3$-ZnO/Y-zeolite against *Escherichia coli* and *Staphylococcus aureus*

Table 2. Antibacterial test results against *Escherichia coli* and *Staphylococcus aureus*

Sample	Diameter of inhibition zone (mm) ± SD		Antibacterial strength
	Escherichia coli	***Staphylococcus aureus***	
$CaCO_3$-ZnO 1:1	3.25 ± 0.05	4.70 ± 0	Weak
$CaCO_3$-ZnO 2:1	0.70 ± 0.07	2.10 ± 0	Weak
$CaCO_3$-ZnO 1:2	5.9 ± 0.07	6.60 ± 0.5	Medium
$CaCO_3$-ZnO/Y-zeolite 2.5 %	7.62 ± 0.74	6.56 ± 0.20	Medium
$CaCO_3$-ZnO/Y-zeolite 5 %	6.56 ± 0.20	5.50 ± 0.58	Medium
$CaCO_3$-ZnO/Y-zeolite 10 %	5.00 ± 0.56	5.31 ± 0.77	Medium
Negative control	0	0	-

Antibacterial strength criteria:

- Weak: diameter of inhibition zone 5 mm or less
- Medium: diameter of inhibition zone 5 – 10 mm
- Strong: diameter of inhibition zone 10 – 20 mm

Antibacterial Activity Test

The antibacterial activity tests of $CaCO_3$-ZnO and $CaCO_3$-ZnO/Y-zeolite were conducted using the agar-well diffusion method against *Escherichia coli* and *Staphylococcus aureus* bacteria. Measuring the diameter of the inhibition zone or clear zone is used as an indicator of the effectiveness of the sample in inhibiting the activity of bacterial growth [33]. Based on the inhibition zone diameter (**Figure 5**), it can be seen that $CaCO_3$-ZnO and $CaCO_3$-ZnO/Y-zeolite nanocomposites have the ability to inhibit the growth of gram-positive bacteria (*Staphylococcus aureus*) and gram-negative bacteria (*Escherichia coli*). The negative control used distilled water because distilled water is the solvent of the $CaCO_3$-ZnO nanocomposites.

Table 2 shows the antibacterial activity test results of $CaCO_3$-ZnO and $CaCO_3$-ZnO/Y-zeolite nanocomposites against gram-positive and gram-negative bacteria. In the nanocomposite before modification, $CaCO_3$-ZnO with a ratio of 1:2 has the largest inhibition zone diameter of 6.6 mm against gram-positive bacteria and 5.9 mm against gram-negative bacteria. After being modified with Y-zeolite, the $CaCO_3$-ZnO nanocomposite with the addition of 2.5 % Y-zeolite has the largest inhibition zone diameter of 6.56 mm against gram-positive bacteria and 7.62 mm against gram-negative bacteria. Based on the inhibitory strength category, $CaCO_3$-ZnO and $CaCO_3$-ZnO/Y-zeolite have antibacterial properties with medium strength against the bacteria. The nanocomposites are bacteriostatic because they only inhibit the growth rate of bacteria [34].

Unmodified $CaCO_3$-ZnO nanocomposite showed better inhibition against gram-positive bacteria. This could be due to differences in cell wall structure in bacteria. Gram-positive bacteria are composed of a thick peptidoglycan layer and teichoic acid, while gram-negative bacteria are composed of a thin peptidoglycan layer. Teichoic acid and lipoteichoic acid in gram-

Table 3. Literature comparison of antibacterial activity of $CaCO_3$-ZnO/Y-zeolite nanocomposite

Material	Antibacterial activity test method	Diameter of inhibition zone (mm)		Reference
		Staphylococcus aureus	***Escherichia coli***	
CaO nanoparticle	Agar-well diffusion	3.3	2.25	[40]
CaO nanoparticle	Agar-well diffusion	5	-	[41]
ZnO nanoparticle	Agar-well diffusion	6,13	resisten	[42]
CuO-ZnO nanocomposite	Disc	2.1	2.3	[14]
$CaCO_3$-ZnO nanocomposite	Agar-well diffusion	6.6	5.9	Current research
$CaCO_3$-ZnO/Y-zeolite nanocomposite	Agar-well diffusion	6.56	7.62	Current research

positive bacteria are sources of negative cell wall charges that facilitate the attachment of positive charges. The negative charge causes positively charged ions such as Ca^{2+} and Zn^{2+} to attach and penetrate the bacterial cell membrane. Research conducted by Wattimena et al. [35] shows that the inhibitory activity of Ag nanoparticles on bacterial growth is related to the release of positive ions. Positive ions can interact with the negative charge of the plasma membrane and stimulate the formation of reactive oxygen species (ROS), causing damage and the death of bacterial cells. Although the peptidoglycan layer in gram-negative bacteria is thin, it contains an outer membrane. This outer membrane consists of lipopolysaccharide (LPS), which is important for the integration of bacterial structures. The lipopolysaccharide layer on the outer membrane can be an obstacle to antimicrobial substances, causing gram-negative bacteria to be more resistant to antibacterial agents [36].

The $CaCO_3$-ZnO nanocomposite, with the addition of 2.5 % Y-zeolite, showed better inhibitory activity against gram-negative bacteria. This could be due to differences in cell wall structure in bacteria. Y-zeolite can loosen the lipopolysaccharide layer on gram-negative bacteria and facilitate the penetration of metal ions so that zeolite particles and Ca^{2+} and Zn^{2+} metal ions easily enter the bacterial cells. In addition, Y-zeolite also has a strong adsorption ability, so it can attract and bind important molecules in bacteria and interfere with their performance. Gram-positive bacteria have a thick peptidoglycan layer with complex cell walls, so Y-zeolite is not easily absorbed into bacterial cells. This causes gram-positive bacteria to be more resistant to antibacterial agents [37].

The antibacterial activity of $CaCO_3$-ZnO and $CaCO_3$-ZnO /Y-zeolite nanocomposites is related to the crystal size produced. Based on the results, it can be seen that the antibacterial activity of $CaCO_3$-ZnO and $CaCO_3$-ZnO /Y-zeolite nanocomposites increases along with the smaller crystal size produced. The nanoscale crystal size will facilitate molecules to penetrate and damage the cell membrane of bacteria. The mechanism of nanocomposites as antibacterials is to interact with bacterial membranes, which causes changes in permeability and damage to bacterial membranes to inhibit bacterial growth [38]. In addition, the antibacterial activity of $CaCO_3$-ZnO may be due to the formation of superoxide and other reactive oxygen species (ROS), such as H_2O and H_2O_2 from the surface of $CaCO_3$-ZnO, which produce free radicals that damage the bacterial cell membrane [39]. ROS generated on the surface of nanocomposites can cause oxidative stress by damaging cell membranes, DNA, and cellular proteins so that antibacterial activity increases [36].

Table 3. shows the comparison of antibacterial activity. The results showed that the combination of two materials with the addition of a stabilizer has better antibacterial activity compared to pure nanoparticles. These results are in accordance with previous study that ZnO-MgO nanocomposite is better at preventing bacterial growth than pure ZnO and MgO nanoparticle [12]. The agar-well diffusion method chosen in this study showed a better bacterial growth inhibition zone compared to the disc method because the sample had an efficient osmosis process so it could effectively inhibit bacterial growth [18].

4. CONCLUSIONS

Y-zeolite-modified $CaCO_3$-ZnO nanocomposites have been successfully synthesized using coprecipitation and impregnation methods. The FTIR spectra obtained showed the presence of carbonate, metal oxide, and zeolite Y groups, interpreting the $CaCO_3$-ZnO/Y-zeolite nanocomposite. The average crystal size of $CaCO_3$-ZnO/Y-zeolite was 35.46-36.53 nm, with crystallinity 35.03-37.66 %. The surface morphology of $CaCO_3$-ZnO/Y-zeolite nanocomposite formed resembles cubes particles with uneven and irregular sizes. EDX results confirmed the presence of $CaCO_3$, ZnO, and Y-zeolite with different elemental percentages. The antibacterial activity test showed that the $CaCO_3$-ZnO nanocomposite was better at inhibiting the growth of gram-positive bacteria (*Staphylococcus aureus*). In comparison, the $CaCO_3$-ZnO/Y-zeolite nanocomposite was better at inhibiting the growth of gram-negative bacteria (*Escherichia coli*). $CaCO_3$-

ZnO/Y-zeolite nanocomposite has the potential to be an antibacterial agent with medium strength. In further research, the $CaCO_3$-ZnO nanocomposite will be modified with natural materials to investigate its antibacterial activity further.

ACKNOWLEDGMENTS

This research was funded by DIPA FMIPA Universitas Negeri Semarang 2023 with the following numbers: 28.1.17.5/UN37/PPK.04/2023.

REFERENCES

1. Khan, Mazumdar A, Pathak S, et al. Biointerfaces Biogenic Ag/CaO Nanocomposites Kill Staphylococcus aureus with Eeduced Toxicity Towards Mammalian Cells. *Colloids Surfaces B Biointerfaces*. 2020;189(November 2019):110846. doi:10.1016/j.colsurfb.2020.110846
2. Khan, Khan QU, Tahur K, et al. A Tagetes minuta based Eco-benign Synthesis of Multifunctional Au/MgO Nanocomposite with Enhanced Photocatalytic, antibacterial and DPPH Scavenging Activities. *Mater Sci Eng C*. 2021;126:112146. doi:10.1016/j.msec.2021.112146
3. Jan T, Azmat S, Mansoor Q, et al. Superior Antibacterial Activity of ZnO-CuO Nanocomposite Synthesized by a Chemical Co-precipitation Approach. *Microb Pathog*. 2019;134(December 2018):103579. doi:10.1016/j.micpath.2019.103579
4. Hong D, Cao G, Qu J, Deng Y, Tang J. Antibacterial Activity of Cu2O and Ag Co-modified Rice Grains-like ZnO Nanocomposites. *J Mater Sci Technol*. 2018;34(12):2359-2367. doi:10.1016/j.jmst.2018.06.011
5. Jayaseelan C, Rahuman AA, Kirthi AV, et al. Novel Microbial Route to Synthesize ZnO Nanoparticles using Aeromonas Hydrophila and Their Activity Against Pathogenic Bacteria and Fungi. *Spectrochim Acta - Part A Mol Biomol Spectrosc*. 2012;90(June):78-84. doi:10.1016/j.saa.2012.01.006
6. Prasetya YA, Nisyak K, Hisbiyah A. Aktivitas Antibakteri dan Antibiofilm Nanokomposit Seng Oksida-Perak (ZnO-Ag) Dengan Minyak Cengkeh terhadap Pseudomonas aeruginosa. *J Bioteknol Biosains Indones*. 2021;8(2):196-207. doi:10.29122/jbbi.v8i2.4770
7. Musdalifa, Purnama MNK, Herawati. Sintesis dan Karakterisasi Nanopartikel Seng Oksida (ZnO) dan Aplikasinya sebagai Agen Antibakteri Staphylococcus aureus pada Kain Katun Jenis Cotton Combed. *Indones J Fundam Sci*. 2019;5(1):15-25.
8. Lailiyah Q, Baqiya MA. Pengaruh Temperatur dan Laju Aliran Gas CO 2 pada Sintesis Kalsium Karbonat Presipitat dengan Metode Bubbling. *J Sains dan Seni ITS*. 2012;1(1).9. Kumar LS, Shantha V, Naik C, Singh CR, Hariharan P. Synthesis , characterization and antibacterial studies of calcite-zincite nanoparticles. *Mater Today Proc*. 2021;46:2520-2527. doi:10.1016/j.matpr.2021.01.644
10. Ariono CD. Sintesis Kalsium Karbonat Presipitat. *EKSERGI*. 2008;9(1):11-15.
11. Abeywardena MR, Elkaduwe RKWHMK, Karunarathne DGGP, et al. Surfactant assisted synthesis of precipitated calcium carbonate nanoparticles using dolomite: Effect of pH on morphology and particle size. *Adv Powder Technol*. 2020;31(1):269-278. doi:10.1016/j.apt.2019.10.018
12. Rompis J, Aritonang H, Pontoh J. Sintesis Nanokomposit ZnO-MgO dan Analisis Efektivitas sebagai Antibakteri. *Chem Prog*. 2020;13(1):56-62. doi:10.35799/cp.13.1.2020.30197
13. Jannah Z, Rohmawati L. Sintesis Nanokristalin CaCO3-MgO untuk Aplikasi Bahan Antibakteri. *J Inov Fis Indones*. 2018;07(2010):11-14.
14. Widiarti N, Sae JK, Wahyuni S. Synthesis CuO-ZnO Nanocomposite and Its Application as an Antibacterial Agent. *J Phys Conf Ser Mater Sci Eng*. 2016;755(1). doi:10.1088/1742-6596/755/1/011001
15. Alswat AA, Bin M, Saleh A. Preparation and Characterization of Zeolite \ Zinc Oxide-Copper Oxide Nanocomposite : Antibacterial Activities. *Colloid Interface Sci Commun*. 2017;16:19-24. doi:10.1016/j.colcom.2016.12.003
16. Munthali MW, Elsheikh MA, Johan E, Matsue N. Proton Adsorption Selectivity of zeolites in Aqueous Media: Effect of Si/Al Ratio of Zeolites. *Molecules*. 2014;19(12):20468-20481. doi:10.3390/molecules191220468
17. Minarti, Budiana A, Ernawati T. Bioaktivitas Turunan Metil Sinamat Terhadap Pertumbuhan Bakteri. *J Kim Val*. 2015;1(1):60-64.
18. Nurhayati LS, Yahdiyani N, Hidayatulloh A. Perbandingan Pengujian Aktivitas Antibakteri Starter Yogurt dengan Metode Difusi Sumuran dan Metode Difusi Cakram. *J Teknol Has Peternak*. 2020;1(September):41-46. doi:10.24198/jthp.v1i2.27537
19. Chen S, Yang Y, Ji M, Liu W. Preparation , characterisation and activity evaluation of CaCO 3 / ZnO photocatalyst. *J Exp Nanosci*. 2011;6(3):324-336. doi:10.1080/17458080.2010.509873
20. Yanti PH, Resmalina R. Facile Chemical Processing of Geloina coaxans Shell and Sodium dihydrogen Phosphate as Precursors to Produce Hydroxyapatite. *J Kim Val*. 2020;6(2):192-197. doi:10.15408/jkv.v6i2.15768
21. Rianto LB, Amalia S, Khalifah SN. Pengaruh Impregnasi Logam Titanium pada Zeolit Alam Malang terhadap Luas Permukaan Zeolit. *Alchemy*. 2012;2(1):58-67. doi:10.18860/al.v0i0.2295
22. Kumar IS, Shantha V, Naik C, et al. Synthesis of calcite-zincite nano composite materials using sol-gel auto combustion method. *Mater Sci Eng*. 2020;1003(1):012132. doi:10.1088/1757-899X/1003/1/012132
23. Yang Z, Xie W. Soybean oil transesterification over zinc oxide modified with alkali earth metals. *Fuel Process Technol*. 2007;88(6):631-638. doi:10.1016/j.fuproc.2007.02.006
24. Mundriyastutik Y, Anggoro DD, Hidayati N, Farmasi P, Kimia T, Diponegoro U. Preparasi dan

Karakterisasi Katalis Como/zeolit Y dengan Metode Pertukaran Ion. *Indones J Farm*. 2016;I(I):28-32.
25. Ma'rifat, Krisdiyanto D, Khamidinal, Nugraha I. Sintesis Zeolite dari Abu Dasar Batu Bara dan Aplikasinya sebagai Adsorben Logam Merkuri (II). *Molekul*. 2014;9(2):73-83.
26. Maharani DK, Hidayah R. Preparasi dan Karakterisasi Komposit Kitosan-ZnO/Al2O3. *Molekul*. 2015;10(1):9-18.
27. Santoso A, Hanindita A, Sumari, Rachman IB. Synthesis of Biodiesel from Low-Quality Crude Palm Oil with Heterogeneous Catalyst Cao-ZnO. *Mater Sci Eng*. 2019;515(1). doi:10.1088/1757-899X/515/1/012082
28. Widianto E, Kardiman, Bayuseno AP, Muryanto S. Identifikasi Struktur Kristal dan Morfologi Endapan Kalsium Karbonat (CaCO3) pada Pipa Tembaga. *Barometer*. 2017;2(2):60-63.
29. Yunita I, Sulistyaningsih T, Widiarti N. Karakterisasi dan Uji Sifat Fisik Material Zeolit Modifikasi Magnetit sebagai Adsorben Ion Klorida dalam Larutan Berair. *Indones J Chem Sci*. 2019;8(2):6-11.
30. Boro J, Thakur AJ, Deka D. Solid oxide derived from waste shells of Turbonilla striatula as a renewable catalyst for biodiesel production. *Fuel Process Technol*. Published online 2011. doi:10.1016/j.fuproc.2011.06.008
31. Rahmawati Z, Holilah H, Purnami SW, Bahruji H, Oetami TP, Prasetyoko D. Statistical Optimisation using Taguchi Method for transesterification of Reutealis Trisperma Oil to Biodiesel on CaO-ZnO Catalysts. *Bull Chem React Eng Catal*. 2021;16(3):686-695. doi:10.9767/BCREC.16.3.10648.686-695
32. Viriya N, Krasae P, Nualpaeng W, Yoosuk B, Faungnawakij K. Biodiesel production over Ca-based solid catalysts derived from industrial wastes. *Fuel*. 2012;92(1):239-244. doi:10.1016/j.fuel.2011.07.013
33. Rohaeti E, Zulaikha NI. Antibacterial Activity of Polyester Fabric with Addition of Hexadecyltrimethoxysilane (HDTMS) against Staphylococcus aureus ATCC 25924. *J Kim Val*. 2017;3(2):95-100. doi:10.15408/jkv.v3i2.5831
34. Marfuah I, Dewi EN, Laras R. Kajian Potensi Ekstrak Anggur Laut (Caulerpa racemosa) sebagai Antibakteri terhadap Bakteri Escherichia coli dan Staphylococcus aureus. *J Peng Biotek Has Pi*. 2018;53(1):1-8. http://www.tfd.org.tw/opencms/english/about/background.html%0Ahttp://dx.doi.org/10.1016/j.cirp.2016.06.001%0Ahttp://dx.doi.org/10.1016/j.powtec.2016.12.055%0Ahttps://doi.org/10.1016/j.ijfatigue.2019.02.006%0Ahttps://doi.org/10.1016/j.matlet.2019.04.024%0A
35. Wattimena SC, Ayuningrum DA, Latuasan LY, Samson E, Patty PJ. Properties of Bio-Silver Nanoparticles Mediated by Tuber and Leaf Extracts of Manihot esculenta. *Biosaintifika*. 2022;14(2):271-278. doi:10.15294/biosaintifika.v14i2.37667
36. Dimapilis EAS, Hsu CS, Mendoza RMO, Lu MC. Zinc oxide nanoparticles for water disinfection. *Sustain Environ Res*. 2018;28(2):47-56. doi:10.1016/j.serj.2017.10.001
37. Salama TM, Ali IO, Gumaa HA, Lateef MA, Bakr MF. Novel Synthesis of Nay Zeolite from Rice Husk Silica: Modification with Zno and Zns for Antibacterial Application. *Chem Sci J*. 2016;07(01). doi:10.4172/2150-3494.1000118
38. Notriawan D, Ernis G, Wibowo RH, Pertiwi R, Malau TR. Aktivitas Antibakteri Nanopartikel Perak Hasil Green Synthesis Menggunakan Ektrak Kulit Buah Kemuning (Murraya Paniculata (L) Jack). *BIOEDUSAINSJurnal Pendidik Biol dan Sains*. 2020;3(2):140-144. doi:10.31539/bioedusains.v3i2.1850
39. Alsohaimi IH, Nassar AM, Seaf Elnasr TA, Cheba B amar. A novel composite silver nanoparticles loaded calcium oxide stemming from egg shell recycling: A potent photocatalytic and antibacterial activities. *J Clean Prod*. 2020;248:119274. doi:10.1016/j.jclepro.2019.119274
40. Ikram M, Saeed M, Haider J, et al. Facile synthesis of chitosan-grafted polyacrylic acid-doped CaO nanoparticle for catalytic and antimicrobial potential. *Appl Nanosci*. 2022;12(9):2657-2670. doi:10.1007/s13204-022-02576-6
41. Aziz DMA, Yousef NMH. Antimicrobial Effects of Calcium Oxide Nanoparticles and Some Spices in Minced Meat. *ARC J Anim Vet Sci*. 2017;3(2):38-45. doi:10.20431/2455-2518.0302004
42. Romadhan M, Suyatma NE, Taqi FM. Synthesis of ZnO nanoparticles by precipitation method with their antibacterial effect. *Indones J Chem*. 2016;16(2):117-123. doi:10.14499/ijc-v16i2p117-123